An Ab Initio Force Field for Predicting Hydrogen Storage in IRMOF Materials

ARTICLE *in* THE JOURNAL OF PHYSICAL CHEMISTRY C · DECEMBER 2009

Impact Factor: 4.77 · DOI: 10.1021/jp907921q

2 AUTHORS, INCLUDING:

Jia Fu
University of California, Riverside
12 PUBLICATIONS **85** CITATIONS

An Ab Initio Force Field for Predicting Hydrogen Storage in IRMOF Materials

Jia Fu and Huai Sun*

School of Chemistry and Chemical Technology, Shanghai Jiao Tong University, Shanghai 200240, China

Received: August 16, 2009; Revised Manuscript Received: October 28, 2009

An ab initio force field that describes interactions between hydrogen molecules and IRMOF materials is proposed. The force field parameters were derived by fitting to ab initio data that includes higher-order electron correction and extended basis-set effects and validated by calculating adsorption isotherms and isosteric heats of adsorption of H_2 in IRMOF-1 using GCMC simulations performed at 77 and 298 K, in a broad range of pressure from 0.0 to 8.0 MPa. Excellent agreements with experimental data were obtained. The force field was then applied to predict hydrogen-storage capacities for eight additional IRMOF materials. It was identified that the void fraction of volume (VFV) has a strong impact on the adsorption capacity, and its impacts on gravimetric and volumetric adsorption uptakes exhibit opposite trends. An overall optimal VFV is ca. 87% for IRMOFs at 77 K and 8.0 MPa.

I. Introduction

Hydrogen storage is a key problem in the research of hydrogen energy sources. Among various options, storage based on physical adsorption using metal−organic framework (MOF) materials[1−9] has drawn considerable attention because their structures can be controlled by varying linkers and metals to reach extremely large surface areas. However, the capacity of hydrogen storage using MOF materials has not met the targeted goal for practical applications yet. The search for new MOF materials is a continuing effort. A general objective is to enhance the interactions between hydrogen molecules and pore surfaces of the materials. Along this direction, various chemical modifications, such as doping with metal ions,[10−12] using unsaturated transition metals,[9,13−15] and replacing the metal elements with nonmetal elements to make covalent organic frameworks (COFs),[16−18] have been reported in the literature.

Among many reported MOF materials,[6,9,19−23] IRMOF-1 (or MOF-5)[1] has been treated as a prototype studied for hydrogen-storage purpose.[6−8,19,20,22,24−26] Along with experimental efforts, computational methods have been used to study how hydrogen molecules are stored in the porous materials and to help design new materials more efficiently. The computational approaches applied to MOFs can be classified into two broad categories: quantum mechanics (QM) calculations and force field based simulations. QM density functional theory (DFT) calculations, with and without periodic condition, have been shown to be successful for predicting molecular and crystal cell structures of MOFs.[27−30] Predicting interaction energies between hydrogen molecules and MOF surfaces is much more challenging. Comprehensive ab initio calculations including high-level electron correlation and extrapolation to complete basis set have been applied.[31−34] Due to extraordinarily high computational demands, most of these calculations were performed on the basis of small cluster models. Recent development extended to larger clusters which were demonstrated resembling the crystal environment.[34] Force field simulations were predominantly done by using the grand canonical Monte Carlo (GCMC) method to predict adsorption isotherms of hydrogen in MOFs.[10,24,35−44] Adsorption isotherm curves and isosteric heats of adsorption have been calculated using simulation techniques.

Ab initio QM calculations are predictive because their accuracy does not depend on knowledge of existing experimental data. However, these calculations are limited to small cluster models, and static energy results can only be remotely correlated to experimental data.[34] On the other hand, results of force field simulations can be directly compared with experimental data, but accuracies of the predictions depend on the quality of underlying force field parameters, which must be thoroughly validated in order to make useful predictions. Most GCMC simulations carried out for studying hydrogen storage on MOFs were based on generic[35−39,41,42] or empirical[45] force fields. The generic force fields have not been validated rigorously for representing interactions between hydrogen molecules and MOFs.[43] Despite some predictions being in good agreement with known experimental data for IRMOF-1,[10,35,36,41,46] controversies such as whether electrostatic terms should be used or not have been raised in the literature. In addition, it is not certain if the same force field parameters can be applied to other materials with the same accuracy. The most useful experimental data, which can be used to parametrize a force field that represents hydrogen and MOF interactions, are adsorption isotherms and enthalpies. Unlike liquid densities and vaporization enthalpies, which are generally easy to measure and available for organic liquids and polymers,[47,48] these properties are difficult to measure accurately and little data are available. It is known that measured adsorption isotherms can be very different for the same material primarily depending on the synthesis and activation conditions.[8] Evidence shows that an empirically derived force field is strongly biased by underlying experimental data and its accuracy is unknown until more accurate experimental data are available.[44,46] Unless the accuracy of the force field is known, the main function of simulation is limited to reproducing known experimental data.

A combination of first-principle calculation and force field simulation can be achieved by developing force field parameters with high quality ab initio data. This approach is of great significance because it takes advantage of both approaches and predicts experimentally measurable data independently. Along this direction, Han et al. has developed the first ab initio force

* To whom correspondence should be addressed. E-mail: huaisun@sjtu.edu.cn.

10.1021/jp907921q
Published on Web 11/11/2009

field for predicting hydrogen storage in MOFs.[10,40] Unfortunately, the QM data used in their parametrization was based on model molecules that were too small to represent interactions between hydrogen molecules and metal oxide clusters according to recently published work.[34] In addition, their force field model did not include the electrostatic terms that are critical for predicting the relative orientations of hydrogen molecules in MOF surfaces. Perhaps due to these causes, the proposed ab initio model has been shown to be flawed in the prediction of adsorption isotherms when it was applied in a broad range of thermodynamic conditions.[44]

In this work, we revisited this subject by utilizing the latest ab initio data[10,31−34] to develop a force field representing the interactions between hydrogen molecule and MOFs accurately. Because of the limitations of computational resources, some of the existing ab initio data was not at the same level of accuracy as others. We carefully examined all ab initio data available to us and made corrections to those "questionable" data sets using reliable data as references. The corrected ab initio data set was used as the only baseline for parametrization. The resulting force field parameters were validated by predicting hydrogen adsorptions in IRMOF-1 under a broad range of thermodynamic conditions. In accordance with force fields developed for hydrogen molecules, we included electrostatic terms in our force field and applied corrections of quantum effects in the simulations. Finally, we applied the same force field parameters to predict adsorption curves for different but similar IRMOFs materials to test the transferability of the proposed force field parameters.

II. Models and Methods

Following the literature,[35,39,49,50] we used the rigid molecular model for both hydrogen molecule and MOFs in this work. Interaction energies between hydrogen and MOF atoms were represented by the pairwise Coulomb and Lennard-Johns (LJ) 12-6 terms:

$$E(r_{ij}) = E_{LJ} + E_{Coul} = 4\varepsilon_{ij}\left[\left(\frac{\sigma_{ij}}{r_{ij}}\right)^{12} - \left(\frac{\sigma_{ij}}{r_{ij}}\right)^{6}\right] + \frac{q_i q_j}{r_{ij}} \quad (1)$$

The Lorentz−Berthelot combination rule was used for construct parameters for different atom pairs.

$$\varepsilon_{ij} = \sqrt{\varepsilon_i \varepsilon_j} \quad \sigma_{ij} = \frac{\sigma_i + \sigma_j}{2} \quad (2)$$

For hydrogen molecules, the Darkrim and Levesque (DL) potential function[51] was used. In the DL model, the H−H bond length is fixed at 0.0741 nm, a LJ interaction site ($\sigma_i = 2.96$ Å and $\varepsilon_i = 0.3051$ kJ/mol) is placed at the center of mass, and three point charges are placed on the nucleus ($q_i = 0.4664$) and the center of mass ($q_i = -0.9328$), representing the quadruple moment of a hydrogen molecule.

For MOF atoms, charge and LJ parameters were derived by fitting ab initio data calculated on model molecules representing fragments of MOFs. Two model molecules, zinc oxide tetrahedron with six formate anion ligands (zinc oxide) and lithium 1,4-benzenedicarboxylate (Li-BDC), were used to represent the zinc oxide connectors and BDC organic linkers in IRMOF-1,[32] respectively (Figure 1). The structures of these model molecules were optimized using DFT with RI-BP86 functional[52−54] and

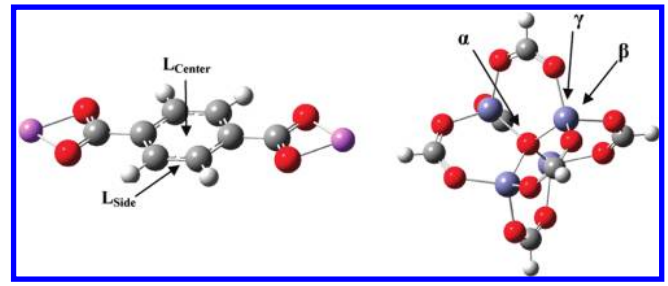

Figure 1. Model compounds representing MOFs in this work. The interactions with hydrogen molecule are sampled along five probe paths indicated by arrows.

TZVPP basis sets.[55] Interaction energies between model and hydrogen molecules were calculated at the RI-MP2/TZVPP level of theory without BSSE correction, using molecular clusters in which the intrastructures of both molecules were fixed. Interaction energies were calculated along five probing paths as illustrated in Figure 1. Two of the sampling paths were used to sample the interactions between hydrogen molecule and BDC toward the center (L_{center}) and side (L_{side}) of the phenyl ring. For the zinc oxide cluster, we calculated energies along three paths toward the cup (α), the ZnO3 (β), and the ZnO2 (γ) sites.[34] A larger model, consisting of both the zinc oxide cluster and the BDC linker,[32,34] was used for calculating the atomic partial charges using the ChelpG[56] method at the B3LYP/6-31+G* level of theory. The QM calculations were carried out with the following program packages: Gaussian 03W[57] for obtaining the ab initio ESP charge data and TURBOMOLE 5.8[58] for calculating the binding energies on various sites.

The quantum effect was included in our simulations semiclassically by using the Feynman−Hibbs (FH) expansion up to the quartic term:[59−61]

$$U_{FH}(r) = U(r) + \frac{\beta\hbar^2}{24\mu}\left[U'(r)' + \frac{2U'(r)}{r}\right] + \frac{\beta^2\hbar^4}{1152\mu^2}\left[\frac{15U'(r)}{r^3} + \frac{4U'''(r)}{r} + U''''(r)\right] \quad (3)$$

where $U(r)$ is the classical potential energy function, μ is the reduced mass of interacting molecules, and $\beta = 1/kT$.

Adsorption isotherms of hydrogen in MOFs were predicted using conventional GCMC[62,63] simulation method. Simulations were performed on unit cells of MOFs under 3D periodic boundary conditions. van der Waals (VDW) interactions were evaluated using 12.9 Å cutoff and compensated with tail corrections. Electrostatic energies were calculated using the Ewald summation. Each of the GCMC simulations included 10^6 moves for equilibration and 10^6 moves for data collection. MC moves included insertions, deletions, translations, and rotations of molecules. Chemical potentials used in the simulations were calculated using the Widom insertion method.[63] The data of each simulation trajectory was divided into 10 blocks in order to estimate uncertainties. MC simulations were carried out using the Towhee 4.16.8 program.[64]

Both absolute adsorption and excess adsorption isotherm curves were calculated. Absolute adsorption weight percent is calculated as

$$wt_{abs}\ \% = \frac{N_{ads} m_{H_2}}{M_{MOF} + N_{ads} m_{H_2}} \times 100\% \quad (4)$$

where N_{ads} is the total number of molecules adsorbed in a unit cell, m_{H_2} is the mole mass of H_2, and M_{MOF} is the mole mass of the unit cell. Excess adsorption weight percent is defined as

$$\mathrm{wt}_{exc}\ \% = \frac{m_{H_2}(N_{ads} - \rho_b V_{free})}{M_{MOF} + m_{H_2}(N_{ads} - \rho_b V_{free})} \times 100\% \quad (5)$$

where ρ_b is the bulk gas number density at the same temperature and pressure of simulation and V_{free} is the MOF free volume accessible to the adsorbates.[35] Volumetric adsorption (g/L) is defined as

$$V_{ads} = \frac{N_{ads} m_{H_2}}{V_{MOF}} \quad (6)$$

We also calculated the effective gravimetric weigh percent,[22] which is defined as

$$\mathrm{wt}_{eff}\ \% = \frac{m_{H_2}(N_{ads} - \rho_b V_{MOF})}{M_{MOF} + m_{H_2}(N_{ads} - \rho_b V_{MOF})} \times 100\% \quad (7)$$

where V_{MOF} is the volume of the unit cell. This quality measures how many additional molecules are stored in a space filled with adsorbents in comparison with the same space without adsorbents.

Isosteric heat of adsorption was calculated using the fluctuations of a quantity involving a number of adsorbate molecules N and the potential energy U:[65]

$$Q_{st} = -\frac{\langle NU\rangle - \langle N\rangle\langle U\rangle}{\langle N^2\rangle - \langle N\rangle^2} + RT \quad (8)$$

These fluctuations were calculated from the energy and particle number trajectories of simulations under different pressures and fixed temperature (77 K). To compare with experimental data, calculated results were expressed as functions of adsorption amounts.

III. Results and Discussion

1. Ab Initio Data. RI-MP2/TZVPP energy curves calculated for interaction between hydrogen molecule and model molecules of IRMOF-1 along five probe paths are displayed in Figures 2−6. Since our calculations lacked correction for higher-order electron correlation and were limited by the basis set, we surveyed the literature for advanced calculation data, the results of which are listed in Table 1.

For the H_2/$BDCLi_2$ model, scanned energy curves show that the most stable configuration corresponds to a hydrogen molecule perpendicularly positioned toward the center of the benzene ring (L_{center}) with distance of ca. 3.0 Å between the centers of mass (COM) of two molecules and binding energy of −5.5 kJ/mol. For configurations in which the hydrogen molecule is parallel to the benzene ring, the binding energies are about 1.5 kJ/mol weaker. Interactions on the side of the phenyl ring (L_{side}) are much weaker, in the vicinity of −1.5 kJ/mol. Hübner et al.[31] studied the interaction of hydrogen molecule with a series of aromatic molecules including $BDCLi_2$. They reported that the energy data obtained using the RI-MP2 method and TZVPP basis set with counterpoise (CP) correction

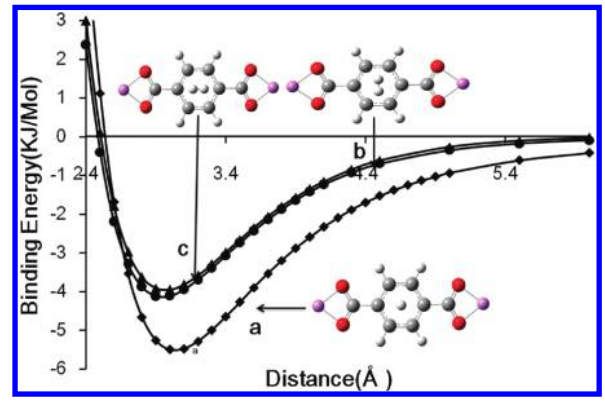

Figure 2. The H_2−$BDCLi_2$ interaction energy curves calculated at the RI-MP2/TZVPP level of theory. Hydrogen molecule is on the top of benzene ring (L_{center}) in perpendicular (a) and parallel (b, c) positions with respect to the ring plane. The separations are measured by the centers of masses.

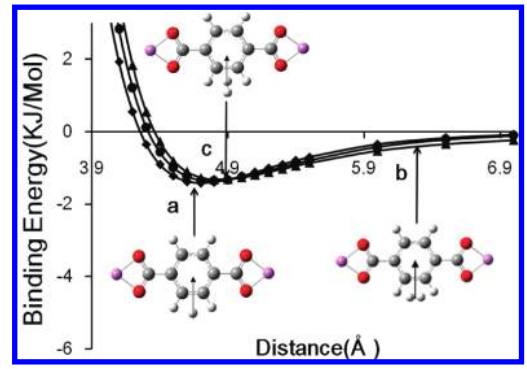

Figure 3. The H_2−$BDCLi_2$ interaction energy curves calculated at the RI-MP2/TZVPP level of theory. Hydrogen molecule is on side of benzene ring (L_{side}), in (a) cross, (b) parallel, and (c) perpendicular positions to the side C−C bond. The separations are measured by the centers of masses.

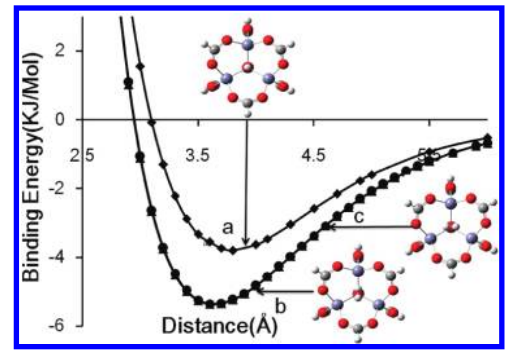

Figure 4. The hydrogen molecule and zinc oxide cluster interaction energy curves calculated for the α site at the RI-MP2/TZVPP level of theory. The hydrogen molecule is (a) perpendicular and (b, c) parallel to the Zn3 plane. The separations are measured by centers of masses.

of the basis set superposition error (BSSE) were very close to those obtained using CCSD(T) methods that include the higher-order electron correlation (HEC) effects and extrapolated to near-complete basis sets (CBS). For $BDCLi_2$, the binding energy was estimated to be 4.30 kJ/mol. Using large (aug-cc-pVTZ and aug-cc-pVQZ) basis sets and estimated CBS limit, Sagara et al.[32] obtained a binding energy of 5.41 kJ/mol. Results obtained with RI-MP2/QZVPP methods were similar; however, after adding CCSD(T) and considering charge-transfer corrections, the value was reduced to 4.16 kJ/mol,[33] which was very close to that reported by Hübner et al.[31] Han et al.[10] calculated the binding

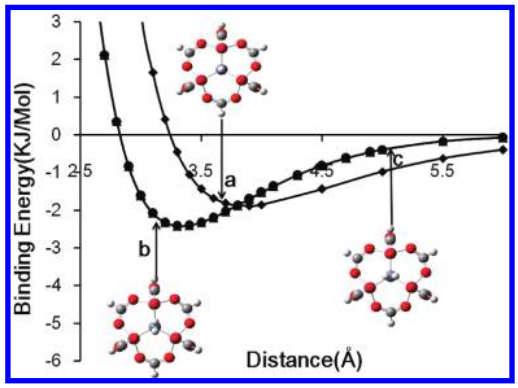

Figure 5. The hydrogen molecule and zinc oxide cluster interaction energy curves calculated for the β site at the RI-MP2/TZVPP level of theory. The hydrogen is (a) perpendicular and (b, c) parallel to the O3 plane. The separations are measured by the center of mass of hydrogen and the closest zinc atom.

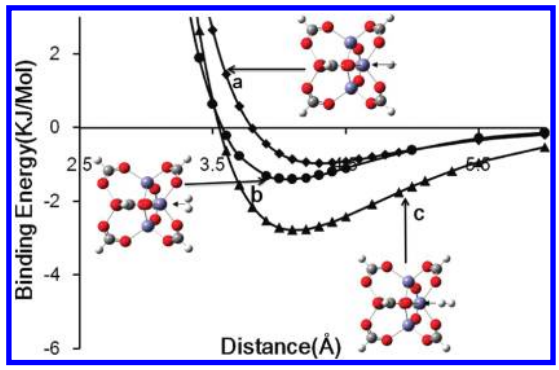

Figure 6. The hydrogen molecule and zinc oxide cluster interaction energy curves calculated for the γ site at the RI-MP2/TZVPP level of theory. The orientations are measured by the axis of hydrogen molecule and the two oxygen atoms of the zinc oxide: (a) cross, (b) parallel, and (c) perpendicular. The separations are measured by the center of mass of hydrogen and the closest zinc atom.

TABLE 1: Comparison of Interaction Energies (in kJ/mol) of Hydrogen Molecule with Model Compounds of MOFs Calculated at Different Theoretical Levels and for Various Binding Sites

ref	note	L_{center}	α	β	γ
Hübner et al.[31]	[a]	4.3			
Sagara et al.[32]	[b]	5.38	6.86		
Sagara et al.[33]	[c]	4.16			
Han et al.[10]	[d]	3.8	6.2		
Sillar et al.[34]	[e]	5.1	8.0	4.6	5.2
Sillar et al.[34]	[f]	4.8	7.6	4.4	5.0

[a] Calculated with $BDCLi_2$ model at the RI-MP2/TZVPP level of theory with BSSE correction. [b] $BDCLi_2$ model for the L site and formate zinc oxide model for the α site, calculated at the level of MP2/cc-pVDZ(SVP for Zn) and MP2/aug-cc-pVTZ (TZVP for Zn) and CBS estimate. [c] Calculated using the $BDCLi_2$ model at the RI-MP2/QZVPP//RI-MP2/TZVPP level of theory method with CCSD(T) correction, no BSSE correction. [d] The binding energy for the α site was calculated using the formate model optimized at the RI-MP2/TZVPP and calculated with RI-MP2/QZVPP method without BSSE correction. The L site was calculated with benzene model, using RI-MP2/TZVPP method, with BSSE correction. [e] Calculated using benzoate models at the level of MP2/CBS(D,T)//MP2/def2-TZVP level, with extrapolation to complete basis set. [f] CP-corrected MP2/aug-cc-pVTZ//MP2/def2-TZVP, without extrapolation to complete basis set.

energy of a hydrogen molecule with benzene using RI-MP2/TZVPP methods and CP correction, obtaining a value of 3.8 kJ/mol. Unfortunately, the model molecule was too small, and

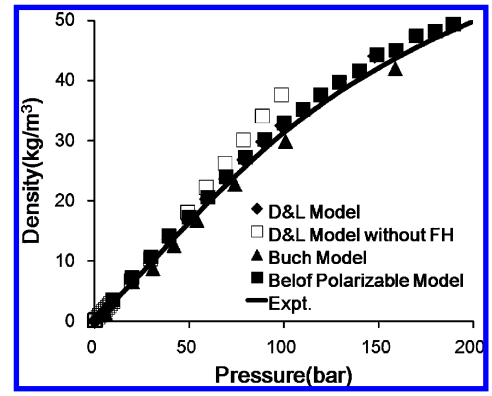

Figure 7. Comparison of simulated and experimental densities of bulk H_2 at 77 K. The dots represent calculated data using different force fields, and the line represents experimental data.

these authors did not explore the corrections of CBS and HEC. Very recently, Sillar et al. carried out the most extensive RI-MP2 calculations to date using large model molecules.[34] These authors reported the interaction energies between a hydrogen molecule and the L site calculated at the CP-corrected MP2/aug-cc-pVTZ level of theory (optimized at MP2/def2-TZVP level), and the CBS correction was 5.1 kJ/mol. These authors pointed out that including HEC would reduce the binding energies by 0.75 kJ/mol,[34] which leads to similar results as reported by Hübner et al.[31]

For the α site of the zinc oxide cluster, the binding energy we obtained for the most stable configuration is −5.4 kJ/mol, which corresponds to hydrogen molecule parallel to the Zn3 plane. When the hydrogen is perpendicular to the Zn3 plane, the binding energy is about 2 kJ/mol weaker. In the most stable configuration, the distance between the COMs of the hydrogen and zinc oxide molecule is 3.6 Å. The binding energy obtained at the MP2/cc-pVDZ(SVP for Zn) level with CBS correction by Sagara et al.[32] was −6.86 kJ/mol. At the RI-MP2/QZVPP//TZVPP level without CP correction, Han et al. obtained the binding energy of −6.2 kJ/mol. Using a large "benzoate" model, Sillar et al.[34] predicted −7.6 kJ/mol with CP-corrected MP2/aug-cc-pVTZ calculation and −8.0 kJ/mol with CBS correction. These authors reported that the −7.6 kJ/mol interaction energy is reduced to −5.4 kJ/mol using the formate model.[34]

The most stable configuration on the β site (the b curve in Figure 5) is with the hydrogen molecule parallel to the O3 plane. An alternative perpendicular configuration is slightly weaker in binding energies. For the γ site, the three energy curves are quite different. The most stable one (Figure 6c) positions the hydrogen molecule perpendicular to the O2 axes. Our binding energy data calculated for the most stable configurations at β and γ sites at the RI-MP2/TZVPP level were −2.5 and −2.9 kJ/mol. Both are ca. 2 kJ/mol lower than the data reported by Sillar et al.[34] Since the shortest distances between hydrogen molecules at the β and γ sites and the benzene rings in the benzoate model are about 3 Å, we assume the differences of ca. 2 kJ/mol were due to omitting these benzene rings in our model.

2. Parameterization. We validated the DL potential model by calculating density curves of compressed hydrogen at 77 K and at pressures ranging from 0 to 20 MPa. The FH effective potential was applied by fitting a LJ 12-6 function form to the energy curves calculated using eq 3 at distances ranging from 2.5 to 10 Å. Calculated data is compared with the experimental curve[66] and other calculated curves[24,67] in Figure 7. Results calculated using the DL−FH model agree very well with the

TABLE 2: Unscaled and Best-Estimated Ab Initio Interaction Energies and Force Field Predicted Interaction Energies for Hydrogen Molecule on Various Binding Sites of the IRMOF-1 (in kJ/mol)[a]

site	L_{center}	α	β	γ
ref 34	5.1	8.0	4.6	5.2
scaled	4.3	6.7	3.9	4.4
force field	4.3	6.7	3.3	5.0

[a] The force field data were calculated on unit cell with 3D periodic conditions.

TABLE 3: Atom Types and Optimized LJ (12−6) Parameters for IRMOFs

type	definition	σ (Å)	ε (kJ/mol)
OZn4	tetrahedron oxygen in zinc oxide	3.30	0.54
OCO	carboxyl oxygen	3.50	0.42
ZnO4	tetrahedron zinc in oxide	3.00	0.59
CCO2	carboxyl carbon	3.10	0.30
C∼C2H	aromatic (benzene) carbon	3.05	0.55
C∼C2C	aromatic carbon bonded to carboxyl	2.80	0.48
HC	hydrogen bonded to aromatic carbon	2.20	0.18

TABLE 4: Charge-Increment Parameters for Atom Pairs in IRMOFs

atom pair	ΔQ
OZn4−ZnO4	0.481
OCO−ZnO4	0.343
OCO−CCO2	0.374
CCO2−C∼C2C	0.105
C∼C2C−C∼C2H	0.006
C∼C2H−HC	0.148

experimental data and are very close to those obtained using the polarizable potential recently developed by Belof et al.[67] Data calculated using the Buch model[24] with FH correction appears to be slightly underestimated, but with similar accuracy to other models.

Seven atom types were defined for atoms in MOFs using calculated atomic partial charges as a guidance. The charge-increment parameter that measures the amount of charge transfer between two bonded atoms was used to represent atomic partial charge distributions. For the seven atom types, six charge-increment parameters were adjustable and determined by fitting to the ab initio ESP charges. The resulting charge-increment parameters are listed in Table 4.

As all parameters of hydrogen molecule and charge parameters of MOF atoms were fixed, the remaining unknown parameters were only the LJ parameters for MOF atoms. Since our RI-MP2/TZVPP calculations did not include HEC and CBS corrections and the model molecules were not sufficiently large to represent the MOF crystal environment, we derived the LJ parameters for MOF atoms in two steps. First, we obtained a set of initial parameters by fitting hydrogen−MOF interaction energies calculated at the RI-MP2/TZVPP level of theory for clusters; we then optimized these parameters by matching calculated binding energies of hydrogen molecule in the IRMOF-1 unit cell with the best ab initio data available.

In the first step, 416 energy data points were used to fit the 14 LJ parameters for seven atom types. The ratio of data points and parameters was approximately 30:1. Despite the simple functional form and very complex potential energy surfaces, the fit was reasonably satisfactory. In a range from −5.50 to 13.16 kJ/mol, the unsigned average deviation between the force field and ab initio data was 0.26 kJ/mol and the rmsd deviation was 1.08 kJ/mol.

To optimize the LJ parameters, we established a set of baseline data by careful examination of available ab initio data. As discussed above, binding energy data obtained for the L_{center} site were consistently around ca. 4.2−4.3 kJ/mol among different research groups.[31,33,34] For sites on the zinc oxide cluster, data were very sparse due to prohibitive computational demands. The binding energy predicted by Sillar et al.[34] of 8.0 kJ/mol for the α site included CBS corrections and contributions from the benzene rings (ca. 2 kJ/mol). The unresolved question is how much the HEC effect contributes. Sillar et al. estimated the correction using CCSD(T) methods on a formate model and obtained a minimal increase in binding energy. A test using the uncorrected energy data to optimize the LJ parameters indicated that the adsorption isotherms and isosteric heat of adsorption were systematically overestimated for hydrogen in IRMOF-1. Considering that the phenyl rings contribute significantly to the interaction energies for hydrogen molecule at the α, β and γ sites and that a 0.75 kJ/mol decrease in the interaction energy was attributed to the HEC effect at the L_{center} site, we suspected that a sizable deduction would be obtained if CCSD(T) calculations were performed on the benzoate model. Unfortunately, the computational demands of such calculations were too high to be carried out. In order to test our hypothesis, we reduced the energy data for the α, β, and γ sites uniformly by using a scaling factor that was the ratio of the binding energies calculated for the L_{center} site with and without HEC correction (4.3/5.1). The scaled binding energies are listed in Table 2.

Sillar et al. compared the binding energy data calculated for hydrogen molecules in the benzoate model and in a unit cell of IRMOF-1 and reported that the differences between cluster and periodic calculations were negligible.[34] Therefore, we used the scaled ab initio binding energy data as baseline data to optimize the LJ parameters of MOF atoms by matching the calculated binding energies of hydrogen molecule in crystalline IRMOF-1. The interaction energies calculated using the optimized force field parameters are listed in Table 2. The calculated data match the baseline data very well for L_{center} and α sites but not very well for β and γ sites. The energy is underestimated for the β site and overestimated for the γ site; this discrepancy presumably indicates that energy function surfaces are more complicated than the simple LJ function can represent. However, the total binding energy of the β and γ sites, weighted by the number ratio (1:3) of the two sites in unit cell, is in close agreement with the ab initio data.

3. Validation on IRMOF-1. Figure 8 displays a comparison of predicted isotherm curves using the force field developed in this work for hydrogen uptake in IRMOF-1 at pressures ranging from 0 to 0.1 MPa at 77 K. Our calculated adsorption curve agrees very well with experimental results.[19,68] The prediction using parameters optimized on the basis of the unscaled energy data of Sillar et al.[34] significantly overestimates the isotherm curve.

Han et al.[10] calculated the isotherm at this temperature and pressure range and their predictions were in good agreement with experimental data. Garberoglio et al.[35] reported predictions using UFF and DL force fields (without QM effect) were significantly overestimated and attributed the problem to atomic charges used in the force fields. However, Belof et al.[41] applied

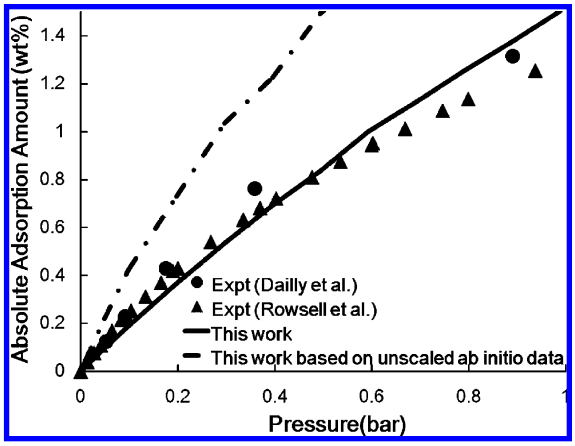

Figure 8. Comparison of simulated (lines) and experimental (dots) hydrogen adsorption isotherms on IRMOF-1 at 77 K in the low-pressure range. In comparison with experimental data, the simulated results using force field derived from unscaled ab initio data[34] are systematically too high.

a polarizable charge model for hydrogen molecule and UFF for IRMOF-1 and obtained excellent agreement with the experimental data. It is well-known that the structure of hydrogen and benzene clusters is determined mainly by quadruple−quadruple interactions. Without electrostatic terms, it is difficult to predict correct structures of hydrogen molecules on MOF surfaces. Since the DL model accurately represents hydrogen−hydrogen interactions as shown in Figure 7, we argue that it is not the charges used in the DL model that are inaccurate but the combination of the DL model with UFF force field that causes the problem. In this work, electrostatic and LJ terms are consistent because LJ terms were parametrized with charges included explicitly.

Isotherms from 0.0 to 8.0 MPa at 77 K are displayed in Figure 9a for absolute adsorption and Figure 9b for excess adsorption. Several sets of experimental curves[6,8,19,20,22,26] are given in the figures for comparison. The deviations among different experimental data are significant. Recently, Kaye et al.[8] examined correlations between synthesis conditions and adsorption capabilities. Materials synthesized without being exposed to air adsorb significantly more hydrogen than those synthesized with air exposition. Our predicted curve is between these two experimental curves. Additionally, our calculated data show that the isotherm calculated without FH correction is significantly higher than that calculated with FH correction, indicating the importance of quantum effects.

Excess adsorption curves were calculated using a free volume fraction of 68.6% as suggested by Garberoglio et al.[35] The experimental data[6,8,19,20,22,26] for excess adsorption are widely scattered as well. However, the Kaye's data with and without exposition of air roughly gives upper and lower boundaries. Our prediction, with FH correction, is in the middle of the experimental curves similar to absolute adsorption isotherms. In addition, the experimental curves show maximum excess adsorption amounts around 4 MPa, which reflects the point past which further increasing pressure will not store more hydrogen in the material relative to bulk hydrogen. Our prediction demonstrates a similar curvature with the same maximum point.

The predicted results at 298 K are compared with experimental data[6,8,69,70] in Figure 10. The absolute adsorption curve is in excellent agreement with experimental data.[8] It is interesting to note that quantum effects are still noticeable at this temperature. The excess adsorption isotherms at 298 K are given in Figure 10b accompanied by data from experiments. Our

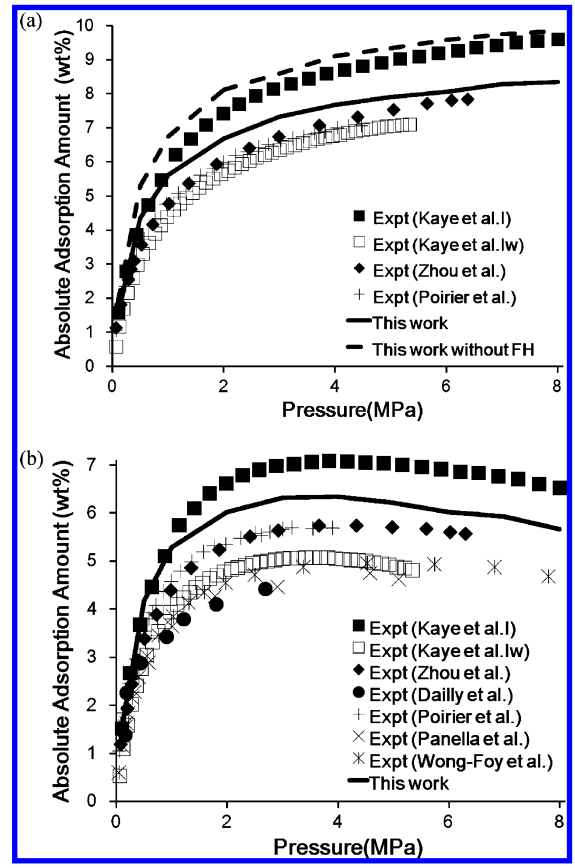

Figure 9. Comparison of simulated (lines) and experimental (dots) adsorption isotherms of hydrogen in IRMOF-1 at 77 K and up to 8 MPa: (a) absolute adsorption and (b) excess adsorption, both in weight percent.

calculated results agree well with those reported by Poirier et al.[70] and Kaye et al.,[8] but the data reported by Li el al.[69] and Panella et al.[6] are significantly lower.

Normalized density maps of adsorbed hydrogen molecules were calculated by accumulating a number of hydrogen molecules in grid space, projected to the $X-Y$ plane and normalized by the total number of adsorbed molecules. The normalized density maps calculated at 0.01 and 8 MPa at 77 K are displayed in Figure 11. At low pressure, hydrogen molecules are concentrated in the vicinity of the zinc oxide connectors with almost none at the center of the unit cell. At high pressure, a noticeable amount can be found in the center and near the organic linkers.[36,39] The normalized density maps of adsorbed hydrogen at 298 K are displayed in Figure 12. Molecules are less concentrated near the metal oxide connectors. It is interesting to note that the relative distributions of hydrogen molecules are essentially the same with different pressures (1 and 8 MPa) at 298 K. This reflects the fact that adsorption at 298 K is mainly determined by volume factors, with interactions between hydrogen molecules and MOF surfaces being of less importance.

As shown in Figure 13, the isosteric heats of adsorption calculated in this work are in the range of 4.2−4.5 kJ/mol, which agree very well with experimental data of ca. 4.0 kJ/mol by Schmitz et al.,[71] 4.1 kJ/mol by Dailly et al.,[19] 4.7 kJ/mol by Rosi et al.,[2] and 4.7−5.2 kJ/mol by Kaye et al.[72] It also shows that the isosteric heats of adsorption calculated using the force field derived from unscaled ab initio data are systematically too high. We list experimental data reported by Zhou et al.[22] in Figure 13 for comparison, because these authors performed measurements over a broad range of temperatures and pressures.

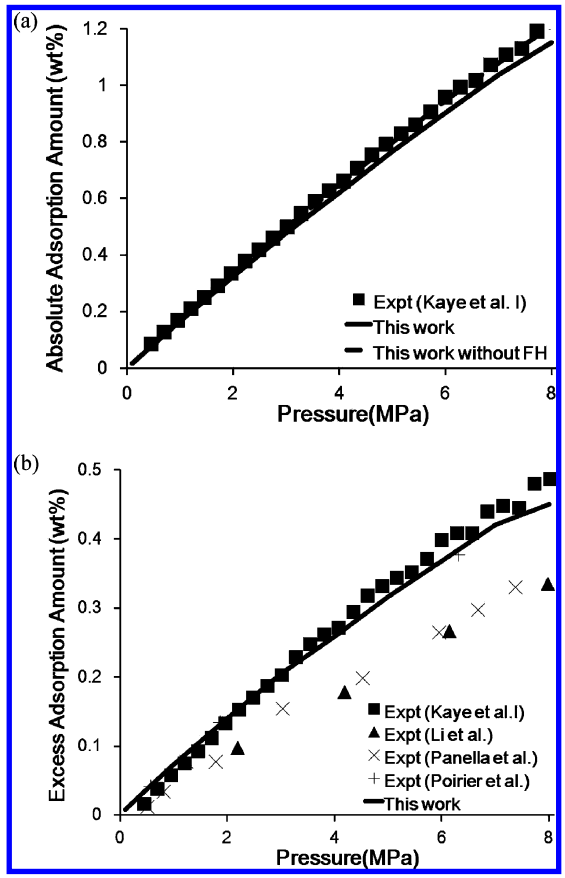

Figure 10. Comparison of simulated (line) and experimental (dots) adsorption isotherms of hydrogen in IRMOF-1 at 298 K, up to 8 MPa: (a) absolute adsorption and (b) excess adsorption, both in weight percent.

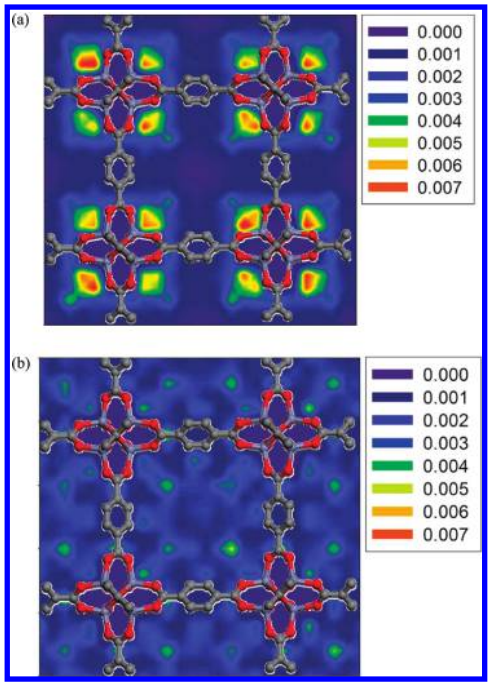

Figure 11. Normalized density projected on the $X-Y$ plane for hydrogen molecules in IRMOF-1 at 77 K and different pressures: (a) 0.01 MPa and (b) 8.0 MPa.

In comparison, our results are slightly lower in the lower load region (<2 wt %) but higher in the higher load region (>2 wt %) than the experimental values of Zhou et al. These discrepancies are likely attributed to differences in experimental and

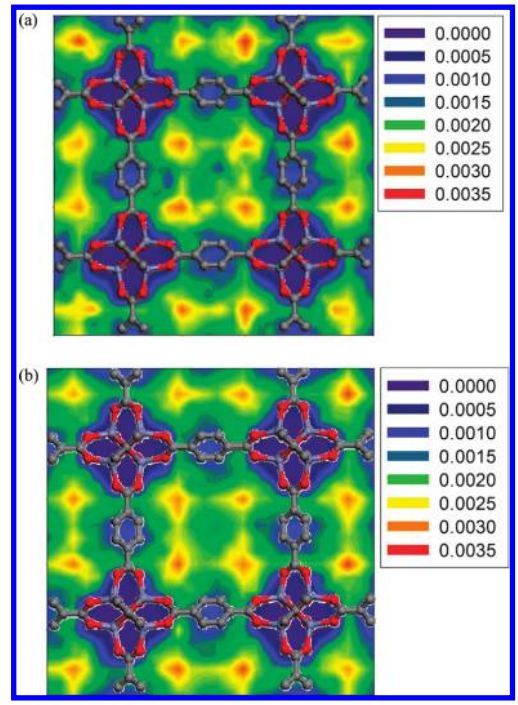

Figure 12. Normalized density projected on the $X-Y$ plane for hydrogen molecules in IRMOF-1 at 298 K and different pressures: (a) 1 MPa and (b) 8.0 MPa.

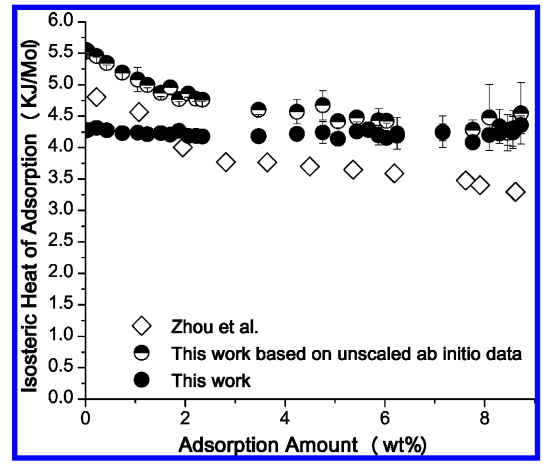

Figure 13. Comparison of simulated and experimental isosteric heat of adsorption for hydrogen in IRMOF-1. The data predicted using force field derived based on unscaled ab initio data are systematically too high.

calculation conditions. The experimental data cited here were obtained by taking finite differentiations of the logarithm of vapor pressure ln(P) with respect to the reciprocal temperature (the Clausius−Clapeyron equation), measured in broad ranges of temperatures from 30 to 300 K and pressures from 0 to 6.5 MPa. In contrast, our calculations were carried out at single temperature of 77 K and a pressure range of 0−8.0 MPa.

4. Extended Predictions. We extended predictions using the same force field parameters to various IRMOF materials that have similar chemical structures: IRMOF-1, IRMOF-8, IRMOF-9, IRMOF-10, IRMOF-13, IRMOF-14, IRMOF-16,[1] MOF-177,[73] and MOF-C30.[40] The simulation cells were constructed using lattice data reported in the literature; the simulations were performed under the same conditions as stated above.

Table 5 lists absolute and excess uptakes in gravimetric adsorption and volumetric adsorption, calculated at three temperatures and 8.0 MPa pressure. As previously reported, none

TABLE 5: Absolute and Excess Gravimetric Adsorption Uptakes and Volumetric Adsorption Uptakes for Different IRMOFs, Calculated at Three Different Temperatures and 8.0 MPa

	298 K			200 K			77 K		
	wt % (abs)	wt % (exc)	g/L	wt % (abs)	wt % (exc)	g/L	wt % (abs)	wt % (exc)	g/L
IRMOF-1	1.15	0.51	6.91	2.24	1.32	13.60	8.34	6.07	54.03
IRMOF-8	1.52	0.60	6.91	2.85	1.54	13.17	10.75	7.66	54.03
IRMOF-9	1.11	0.62	7.36	2.29	1.59	15.36	7.74	6.03	55.09
IRMOF-10	2.04	0.68	6.84	3.61	1.68	12.32	13.41	9.01	50.99
IRMOF-13	0.96	0.59	7.30	2.07	1.55	15.93	6.44	5.12	51.78
IRMOF-14	1.87	0.71	7.11	3.45	1.80	13.34	12.38	8.58	52.76
IRMOF-16	3.09	0.69	6.55	5.14	1.73	11.13	18.01	10.53	45.09
MOF-C30	2.47	0.78	6.94	4.35	1.95	12.46	15.36	10.00	49.74
MOF-177	1.64	0.70	7.12	3.12	1.79	13.75	11.50	8.45	55.46

of the IRMOFs examined was able to meet the U.S. Department of Energy (DOE) targets at room temperature. Frost and Snurr[39] studied the heat of adsorption required to achieve an acceptable gravimetric hydrogen density in MOFs by artificially increasing the interaction potential between hydrogen molecule and MOF atoms in their simulations. Bhatia and Myers[74] deduced the required heat of adsorption based on thermodynamic analysis. Both studies concluded that the isosteric heat of adsorption for hydrogen molecule needed to be 10−15 kJ/mol. This value is far larger than results demonstrated in any MOFs to date, where typical values are between 4 and 10 kJ/mol.[23] Nevertheless, data in Table 5 show that, with different linker moieties, adsorption can be altered significantly. Among those studied, IRMOF-16 shows the greatest adsorption gravimetric capability. It is of interest to point out that the maximum gravimetric adsorption does not correspond to maximum volumetric adsorption capability. Our calculated data show that the greatest volumetric adsorption can be obtained on IRMOF-9.

The gravimetric and volumetric adsorption capacities are correlated with the void fraction of volume (VFV) of MOF volumes, as shown in Figure 14. The VFV was calculated by subtracting the van der Waals volume occupied by MOF atoms in the unit cell from the total volume of the unit cell. As illustrated in the figure, the gravimetric adsorption is exponentially proportional to VFV; on the other hand, volumetric adsorption, except a few data points, is inversely proportional to the VFV. Since both volumetric and gravimetric uptakes are important factors[43] in hydrogen storage, increasing pore volume is not the only factor to be considered in the design of hydrogen-storage materials. As shown in Figure 14, the optimal point that imposes the best overall uptake capacity is located at ca. 87% of VFV, which corresponds to IRMOF-10 among the MOFs we examined under 77 K and 8.0 MPa.

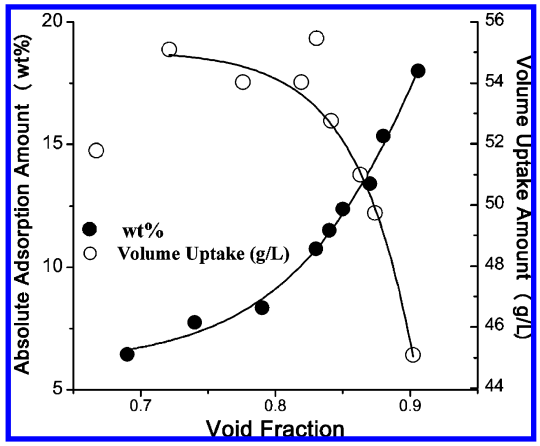

Figure 14. The gravimetric and volumetric uptakes calculated at 77 K and 8.0 MPa are plotted against VFV of IRMOFs. The lines are used to indicate the trends. Generally, the gravimetric uptake exponentially increases, and the volumetric uptake exponentially decreases as the void fraction increases.

For these MOFs, little experimental data about hydrogen adsorption is available for direct comparison. To our best knowledge, Furukawa et al.[21] reported the absolute adsorption amount of 10.2% for MOF-177 at 77 K and 7.2 MPa. Our calculated data of 11.5% at 77 K and 8.0 MPa is in excellent agreement with the experimental data.

Finally, we present the effective adsorption isotherms calculated for various IRMOFs at 77 K in Figure 15. The effective adsorption measures the additional amount of molecules adsorbed in a container with and without the adsorbent. As shown in the figure, the effective adsorption values are positive in the pressure range up to 8.0 MPa at 77 K for all of the MOF materials calculated, which indicates more hydrogen molecules are stored with the adsorbent. Figure 15 also shows that different MOFs demonstrate different maximum efficiency and uptakes, which could be useful for engineering design of storage devices. We did similar calculations at 200 and 298 K; the results were much lower and were all positive values.

IV. Conclusions

This work demonstrated that a force field derived based on ab initio data can be used to predict adsorption isotherms and isosteric heats of adsorption with comparable accuracy to experimental measurements. This approach is promising because it provides a possibility of making accurate predictions before a new material is synthesized.

Developing an accurate force field from first principle calculations is feasible only if the underlying ab initio calculations reach an acceptable accuracy. Because of the weak

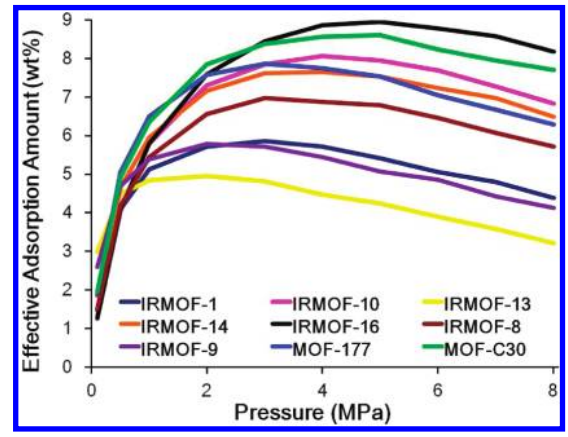

Figure 15. The gravimetric adsorption efficiency curves calculated for different IRMOFs at 77 K.

interactions associated with hydrogen molecules, the basis sets and high-order electron correction effects must be included. In addition, model molecules used in calculations must represent the targeted chemical environment. In this work, we adopted recently published ab initio data. Due to limitation of computational power, the existing ab initio data for the large cluster (benzoate model) had to be corrected. However, this was treated as "ab initio" as possible by scaling all relevant data using a single scaling factor. The scaling factor was not determined by fitting to experimental data but by extrapolating from accurate results calculated for smaller cluster model. Although this scaling cannot be evaluated directly using ab initio calculations, its validity is tested by comparing the simulated adsorption isotherms and enthalpies. As the computer power increases in the future, the uncertainty related to the selection of scaling factor should be resolved.

In comparison with previous efforts, this work shows that electrostatic terms in the force field do not cause problems for representing interactions accurately. It is critical to get consistent representations of both electrostatic and LJ interactions.

Our extended predictions indicate that the force field appears to be transferable among various MOFs with similar chemical constitutions. We demonstrated that pore size, in addition to binding energies, are important factors to be considered for future development of new MOF materials. In particular, VFV has a strong impact on the adsorption capacity, and the impact on gravimetric and volumetric adsorption uptakes exhibits opposite trends. An overall optimal VFV should be ca. 87% for IRMOFs at 77 K and 8.0 MPa.

Acknowledgment. Financial support from the National Science Foundation of China (No. 10676021) and the National Basic Research Program of China (No. 2007CB209701) is gratefully acknowledged.

Supporting Information Available: The RI-MP2/TZVPP energy data of interaction between hydrogen molecule and model molecules of MOFs. This material is available free of charge via the Internet at http://pubs.acs.org.

References and Notes

(1) Eddaoudi, M.; Kim, J.; Rosi, N.; Vodak, D.; Wachter, J.; O'Keeffe, M.; Yaghi, O. M. *Science* **2002**, *295*, 469.
(2) Rosi, N. L.; Eckert, J.; Eddaoudi, M.; Vodak, D. T.; Kim, J.; O'Keeffe, M.; Yaghi, O. M. *Science* **2003**, *300*, 1127.
(3) Dincă, M.; Long, J. R. *J. Am. Chem. Soc.* **2005**, *127*, 9376.
(4) Rowsell, J. L. C.; Spencer, E. C.; Eckert, J.; Howard, J. A. K.; Yaghi, O. M. *Science* **2005**, *309*, 1350.
(5) Dincă, M.; Yu, A. F.; Long, J. R. *J. Am. Chem. Soc.* **2006**, *128*, 8904.
(6) Panella, B.; Hirscher, M.; Pütter, H.; Müller, U. *Adv. Funct. Mater.* **2006**, *16*, 520.
(7) Rowsell, J. L. C.; Yaghi, O. M. *J. Am. Chem. Soc.* **2006**, *128*, 1304.
(8) Kaye, S. S.; Dailly, A.; Yaghi, O. M.; Long, J. R. *J. Am. Chem. Soc.* **2007**, *129*, 14176.
(9) Dincă, M.; Long, J. R. *Angew. Chem., Int. Ed.* **2008**, *47*, 6766.
(10) Han, S. S.; Goddard, W. A. *J. Am. Chem. Soc.* **2007**, *129*, 8422.
(11) Blomqvist, A.; Araujo, C. M.; Srepusharawoot, P.; Ahuja, R. *Proc. Natl. Acad. Sci. U.S.A.* **2007**, *104*, 20173.
(12) Klontzas, E.; Mavrandonakis, A.; Tylianakis, E.; Froudakis, G. E. *Nano Lett.* **2008**, 1572.
(13) Dincă, M.; Dailly, A.; Liu, Y.; Brown, C. M.; Neumann, D. A.; Long, J. R. *J. Am. Chem. Soc.* **2006**, *128*, 16876.
(14) Zhou, W.; Yildirim, T. *J.Phys.Chem.C* **2008**, *112*, 8132.
(15) Liu, Y.; Kabbour, H.; Brown, C. M.; Neumann, D. A.; Ahn, C. C. *Langmuir* **2008**, 4772.
(16) Han, S. S.; Furukawa, H.; Yaghi, O. M.; Goddard, W. A. *J. Am. Chem. Soc.* **2008**, *130*, 11580.
(17) Furukawa, H.; Yaghi, O. M. *J. Am. Chem. Soc.* **2009**, *131*, 8875.
(18) Cote, A. P.; Benin, A. I.; Ockwig, N. W.; O'Keeffe, M.; Matzger, A. J.; Yaghi, O. M. *Science* **2005**, *310*, 1166.
(19) Dailly, A.; Vajo, J. J.; Ahn, C. C. *J. Phys. Chem. B* **2006**, *110*, 1099.
(20) Wong-Foy, A. G.; Matzger, A. J.; Yaghi, O. M. *J. Am. Chem. Soc.* **2006**, *128*, 3494.
(21) Furukawa, H.; Miller, M. A.; Yaghi, O. M. *J. Mater. Chem.* **2007**, *17*, 3197.
(22) Zhou, W.; Wu, H.; Hartman, M. R.; Yildirim, T. *J. Phys. Chem. C* **2007**, *111*, 16131.
(23) Murray, L. J.; Dinca, M.; Long, J. R. *Chem. Soc. Rev.* **2009**, *38*, 1294.
(24) Liu, J.; Culp, J. T.; Natesakhawat, S.; Bockrath, B. C.; Zande, B.; Sankar, S. G.; Garberoglio, G.; Johnson, J. K. *J. Phys. Chem. C* **2007**, *111*, 9305.
(25) Panella, B.; Hönes, K.; Müller, U.; Trukhan, N.; Schubert, M.; Pütter, H.; Hirscher, M. *Angew. Chem., Int. Ed.* **2008**, *47*, 2138.
(26) Poirier, E.; Dailly, A. *J. Phys. Chem. C* **2008**, *112*, 13047.
(27) Fuentes-Cabrera, M.; Nicholson, D. M.; Sumpter, B. G.; Widom, M. *J. Chem. Phys.* **2005**, *123*, 124713.
(28) Mattesini, M.; Soler, J. M.; Yndurain, F. *Phys. Rev. B* **2006**, *73*, 094111.
(29) Braga, C. F.; Longo, R. L. *J. Mol. Struct. THEOCHEM* **2005**, *716*, 33.
(30) Civalleri, B.; Napoli, F.; Noel, Y.; Roetti, C.; Dovesi, R. *Crystengcomm* **2006**, *8*, 364.
(31) Hübner, O.; Gloss, A.; Fichtner, M.; Klopper, W. *J. Phys. Chem. A* **2004**, *108*, 3019.
(32) Sagara, T.; Klassen, J.; Ganz, E. *J. Chem. Phys.* **2004**, *121*, 12543.
(33) Sagara, T.; Klassen, J.; Ortony, J.; Ganz, E. *J. Chem. Phys.* **2005**, *123*, 014701.
(34) Sillar, K.; Hofmann, A.; Sauer, J. *J. Am. Chem. Soc.* **2009**, *131*, 4143.
(35) Garberoglio, G.; Skoulidas, A. I.; Johnson, J. K. *J. Phys. Chem. B* **2005**, *109*, 13094.
(36) Frost, H.; Duren, T.; Snurr, R. Q. *J. Phys. Chem. B* **2006**, *110*, 9565.
(37) Dubbeldam, D.; Frost, H.; Walton, K. S.; Snurr, R. Q. *Fluid Phase Equilib.* **2007**, *261*, 152.
(38) Duren, T.; Millange, F.; Ferey, G.; Walton, K. S.; Snurr, R. Q. *J. Phys. Chem. C* **2007**, *111*, 15350.
(39) Frost, H.; Snurr, R. Q. *J. Phys. Chem. C* **2007**, *111*, 18794.
(40) Han, S. S.; Deng, W.-Q.; Goddard, W. A. *Angew. Chem., Int. Ed.* **2007**, *46*, 6289.
(41) Belof, J. L.; Stern, A. C.; Space, B. *J. Phys. Chem. C* **2009**, *113*, 9316.
(42) Duren, T.; Bae, Y.-S.; Snurr, R. Q. *Chem. Soc. Rev.* **2009**, *38*, 1237.
(43) Han, S. S.; Mendoza-Cortes, J. L.; Goddard, W. A. *Chem. Soc. Rev.* **2009**, *38*, 1460.
(44) Keskin, S.; Liu, J.; Rankin, R. B.; Johnson, J. K.; Sholl, D. S. *Ind. Eng. Chem. Res.* **2009**, *48*, 2355.
(45) Yang, Q.; Zhong, C. *J. Phys. Chem. B* **2006**, *110*, 655.
(46) Yang, Q.; Zhong, C. *J. Phys. Chem. B* **2005**, *109*, 11862.
(47) Jorgensen, W. L.; Maxwell, D. S.; Tirado-Rives, J. *J. Am. Chem. Soc.* **1996**, *118*, 11225.
(48) Sun, H. *J. Phys. Chem. B* **1998**, *102*, 7338.
(49) Liu, J.; Lee, J. Y.; Pan, L.; Obermyer, R. T.; Simizu, S.; Zande, B.; Li, J.; Sankar, S. G.; Johnson, J. K. *J. Phys. Chem. C* **2008**, *112*, 2911.
(50) Han, S. S.; Goddard, W. A. *J. Phys. Chem. C* **2007**, *111*, 15185.
(51) Darkrim, F.; Aoufi, A.; Malbrunot, P.; Levesque, D. *J. Chem. Phys.* **2000**, *112*, 5991.
(52) Perdew, J. *Phys. Rev. B* **1986**, *33*, 8822.
(53) Becke, A. *Phys. Rev. A* **1988**, *38*, 3098.
(54) Eichkorn, K.; Treutler, O.; öhm, H.; Häser, M.; Ahlrichs, R. *Chem. Phys. Lett.* **1995**, *242*, 652.
(55) Schäfer, A.; Huber, C.; Ahlrichs, R. *J. Chem. Phys.* **1994**, *100*, 5829.
(56) Heinz, H.; Suter, U. W. *J. Phys. Chem. B* **2004**, *108*, 18341.
(57) Frisch, M. J.; Trucks, G. W.; Schlegel, H. B.; Scuseria, G. E.; Robb, M. A.; Cheeseman, J. R.; Montgomery, J. A., Jr.; Vreven, T.; Kudin, K. N.; Burant, J. C.; Millam, J. M.; Iyengar, S. S.; Tomasi, J.; Barone, V.; Mennucci, B.; Cossi, M.; Scalmani, G.; Rega, N.; Petersson, G. A.; Nakatsuji, H.; Hada, M.; Ehara, M.; Toyota, K.; Fukuda, R.; Hasegawa, E.; Ishida, M.; Nakajima, I.; Honda, T.; Kitao, O.; Nakai, H.; Klene, M.; Li, X.; Knox, J. E.; Hratchian, H. P.; Cross, J. B.; Adamo, C.; Jaramillo, J.; Gomperts, R.; Stratmann, R. E.; Yazyev, O.; Austin, A. J.; Cammi, R.; Pomelli, C.; Ochterski, J. W.; Ayala, P. Y.; Morokuma, K.; Voth, G. A.; Salvador, P.; Dannenberg, J. J.; Zakrzewski, V. G.; Dapprich, S.; Daniels, A. D.; Strain, M. C.; Farkas, O.; Malick, D. K.; Rabuck, A. D.; Raghavachari, K.; Foresman, J. B.; Ortiz, J. V.; Cui, Q.; Baboul, A. G.; Clifford, S.; Cioslowski, J.; Stefanov, B. B.; Liu, G.; Liashenko, A.; Piskorz, P.; Komaromi, I.; Martin, R. L.; Fox, D. J.; Keith, T.; Al-Laham, M. A.; Peng, C. Y.; Nanayakkara, A.; Challacombe,

M.; Gill, P. M. W.; Johnson, B.; Chen, W.; Wong, M. W.; Gonzalez, C.; Pople, J. A. *Gaussian 03, Revision B.03*; Gaussian, Inc.: Pittsburgh, PA, 2003.

(58) Ahlrichs, R.; Bär, M.; Häser, M.; Horn, H.; Kölmel, C. *Chem. Phys. Lett.* **1989**, *162*, 165.

(59) Feynman, R. P. *Rev. Mod. Phys.* **1948**, *20*, 367.

(60) Feynman, R. P.; Hibbs, A. R. *Quantum Mechanics and Path Integrals*; McGraw-Hill: New York, 1965.

(61) Kumar, A. V. A.; Jobic, H.; Bhatia, S. K. *J. Phys. Chem. B* **2006**, *110*, 16666.

(62) Landau, D.; Binder, K. *A Guide to Monte Carlo Simulations in Statistical Physics*; Cambridge University Press: Cambridge, U.K., 2000.

(63) Allen, M. P.; Tildesley, D. J. *Computer Simulation of Liquids*; Oxford University Press: New York, 1987.

(64) Martin, M. G. MCCCS Towhee, http://towhee.sourceforge.net/, 2006.

(65) Snurr, R. Q.; Bell, A. T.; Theodorou, D. N. *J. Phys. Chem.* **1993**, *97*, 13742.

(66) Lemmon, E.; McLinden, M.; Friend, D. NIST Chemistry WebBook, http://webbook.nist.gov, 2008.

(67) Belof, J. L.; Stern, A. C.; Space, B. *J. Chem. Theory Comput.* **2008**, *4*, 1332.

(68) Rowsell, J. L. C.; Millward, A. R.; Park, K. S.; Yaghi, O. M. *J. Am. Chem. Soc.* **2004**, *126*, 5666.

(69) Li, Y.; Yang, R. T. *J. Am. Chem. Soc.* **2006**, *128*, 8136.

(70) Poirier, E.; Chahine, R.; Benard, P.; Lafi, L.; Dorval-Douville, G.; Chandonia, P. A. *Langmuir* **2006**, *22*, 8784.

(71) Schmitz, B.; Müller, U.; Trukhan, N.; Schubert, M.; Férey, G.; Hirscher, M. *ChemPhysChem* **2008**, *9*, 2181.

(72) Kaye, S. S.; Long, J. R. *J. Am. Chem. Soc.* **2005**, *127*, 6506.

(73) Chae, H. K.; Siberio-Perez, D. Y.; Kim, J.; Go, Y.; Eddaoudi, M.; Matzger, A. J.; O'Keeffe, M.; Yaghi, O. M. *Nature* **2004**, *427*, 523.

(74) Bhatia, S. K.; Myers, A. L. *Langmuir* **2006**, *22*, 1688.

JP907921Q